

Triple Shockley type stacking faults in 4H-SiC epilayers

Gan Feng,^{1,a)} Jun Suda,¹ and Tsunenobu Kimoto^{1,2}

¹Department of Electronic Science and Engineering, Kyoto University, Katsura, Nishikyo, Kyoto 615-8510, Japan

²Photonics and Electronics Science and Engineering Center (PESEC), Kyoto University, Katsura, Nishikyo, Kyoto 615-8510, Japan

(Received 17 December 2008; accepted 13 February 2009; published online 6 March 2009)

4H-SiC epilayers have been characterized by microphotoluminescence (micro-PL) spectroscopy and micro-PL intensity mapping at room temperature. A type of stacking fault (SF) with a peak emission wavelength at 480 nm (2.58 eV) has been identified. The shape of this SF is triangular revealed by the micro-PL intensity mapping. Conventional and high-resolution transmission electron microscopies have been carried out to investigate the structure of this SF. Its stacking sequence is determined as (3,5) in Zhdanov's notation, which is consistent with that of the triple Shockley SF. The formation mechanism of this SF is also discussed. © 2009 American Institute of Physics. [DOI: 10.1063/1.3095508]

Silicon carbide (SiC), as a wide bandgap semiconductor, is an attractive material for developing high-power, high-temperature, and high-frequency devices, owing to its superior properties.¹ However, there are several critical issues related to the crystalline quality (defects) needed to be solved before the full commercialization of SiC devices. Considering that micropipe defects, known to be the most harmful defects for device performance, are no longer a major problem, other defects, particularly various types of stacking faults (SFs) remain a challenge. In recent years, SFs in SiC received increasing attention due to their negative impacts on the performance of 4H-SiC devices and on the long-term operation stability.²

The formation energy of SFs in SiC, e.g., in 4H-SiC, is experimentally determined to be only 14.7 mJ/m² [single Shockley SFs (1SSFs)],³ which is about an order of magnitude lower than the energies of corresponding defects in other semiconductors, such as diamond (280 mJ/m²),⁴ Si (55 mJ/m²),⁵ or GaAs (45 mJ/m²).⁶ Due to the lower formation energy it is relatively easy to generate SFs in 4H-SiC polytype. SFs in 4H-SiC can appear spontaneously during the growth (the bulk and epitaxial growth)^{7,8} or in some later processing steps such as annealing,⁹ oxidation,¹⁰ implantation, or even in electrically stressed *p-i-n* diodes.¹¹ There are several types of SFs reported in 4H-SiC, such as 1SSFs (in degraded *p-i-n* diodes),¹² double Shockley SFs (2SSFs),¹³ in-grown 8H SFs [the stacking sequence is consistent with that of the quadruple Shockley SFs (4SSFs)], so in this letter we will call it 4SSFs,^{7,8} and intrinsic Frank SFs.¹⁴ SFs in 4H-SiC can form quantum-well-like electronic states that emit luminescence. The emission wavelength (energy) is determined by the structure of SFs. 1SSFs and intrinsic Frank SFs show a similar photoluminescence (PL) peak at approximately 420 nm (2.95 eV) at room temperature, while 2SSFs at 500 nm (2.48 eV) and 4SSFs at 455~460 nm (2.70 eV).¹⁵ Another type of SF with an emission wavelength at 480 nm (2.58 eV) was also reported by several groups.¹⁶ However, the structure of that type of SF is still not clear. In this letter, PL and transmission electron microscopy (TEM)

measurements were carried out in order to characterize this unidentified SF.

4H-SiC epilayers were grown on 8° off-axis 4H-SiC (0001) *n*⁺ substrates by horizontal hot-wall chemical vapor deposition in a SiH₄-C₃H₈-H₂ system.¹⁷ Epitaxial growth was performed at 1650 °C with a reactor pressure of 35 Torr and C/Si ratio of 1.3. The growth rate was 50–65 μm/h and the thickness of epilayers was approximately 60 μm. The epilayers were unintentionally doped. Micro-PL spectroscopy and intensity mapping were performed on the samples by using a PLMicro-SiC by Nanometrics Inc. PL was excited by the 25 mW, 325 nm line of a He-Cd laser, dispersed by a grating monochromator, and detected by a photomultiplier. The laser beam was focused to a spot with a diameter of about 0.8 μm using a sapphire objective lens. The sample was mounted on an XYZ stage with a spatial resolution of 0.5 μm. The setup can acquire data in a single wavelength mode (monochromatic PL intensity mapping mode) or in a full spectral scanning mode (PL spectroscopy mode), with the spectral resolution of 1 nm. TEM studies were carried out on a JEOL microscope operating at 300 kV.

Figure 1 shows a room temperature PL spectrum and a monochromatic image (micro-PL intensity mapping) of the SF. At the 4H-SiC matrix (outside the SF), only one peak located at 390 nm with a tail at the low energy side was observed. This peak (3.18 eV) corresponds to the near band-edge emission of 4H-SiC. At the SF position, the intensity of the near band-edge emission is greatly reduced. However, a new band appears with the maximum at 480 nm (2.58 eV). This indicates that the SF manifests itself as an electronic trap in 4H-SiC, in accordance with the quantum well model. The inset of Fig. 1 shows the monochromatic PL intensity mapping at a wavelength of 480 nm. The contrasted color area (triangular shape) corresponds to the SF, which suggests that the 480 nm emission is related to the SF. Characteristically, the intensity of the contrast decreases toward the direction opposite the wafer offcut, i.e., in the direction opposite to the step flow [11 $\bar{2}$ 0]. For SFs residing on the basal planes of 4H-SiC, this corresponds to the increasing distance from the surface of the structure. The energy difference between the band-edge emission and the SF equals to 0.6 eV. Using

^{a)}Electronic mail: gfeng@semicon.kuee.kyoto-u.ac.jp.

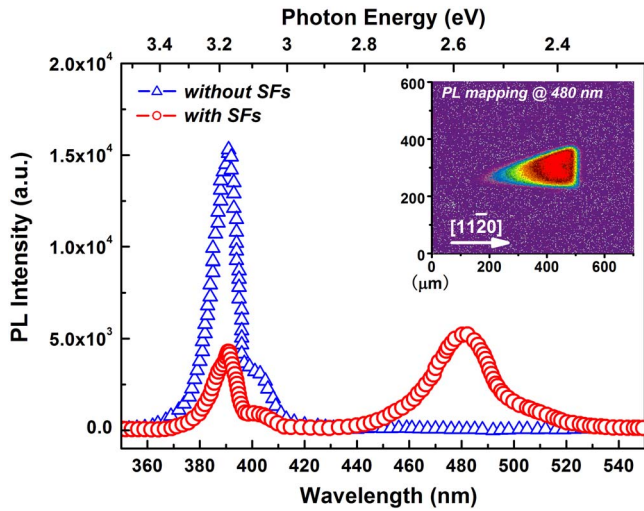


FIG. 1. (Color online) PL spectra of 4H-SiC with and without the SFs. Inset shows the monochromatic micro-PL mapping at wavelength of 480 nm.

ab initio calculations, Iwata *et al.*¹⁸ found that when a 2SSF exists, one single band splits 0.6 eV off below the conduction band minimum. However, the experimental data confirmed that the 2SSFs show the emission wavelength at about 500 nm (2.48 eV, 0.7 eV below the 4H-SiC conduction band minimum). Thus, the structure of the SF with 480 nm must be different from that of the 2SSFs and also differs from other identified SFs. The density of the SFs, which show a 480 nm luminescence, varies from sample to sample, and is typically 1–5 cm⁻². This type of SF is also observed in epilayers grown at a low growth rate of 4 μm/h on 4° off-axis 4H-SiC (0001) substrates. The correlation between the SF density and growth conditions is now under investigation.

We fabricated a cross-sectional TEM sample using focused ion beam micromachining. The sample containing SFs was first etched in molten KOH at 500 °C for 5–10 min. This step produced two etching pits corresponding to two basal plane dislocations and a line corresponding to the intersection of SF with the epilayer surface for each SF, as shown in Fig. 2. The TEM specimens were then cut from the part of the SF where the defect intersected the surface. As shown in Fig. 3(a), in the cross-sectional TEM sample, only

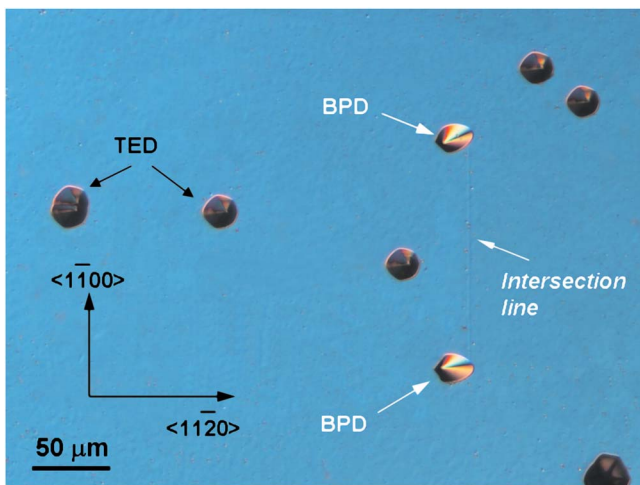


FIG. 2. (Color online) Micrograph of the sample surface after KOH etching. Round-shaped pits represent threading edge dislocations. Oval-shaped pits represent basal plane dislocations.

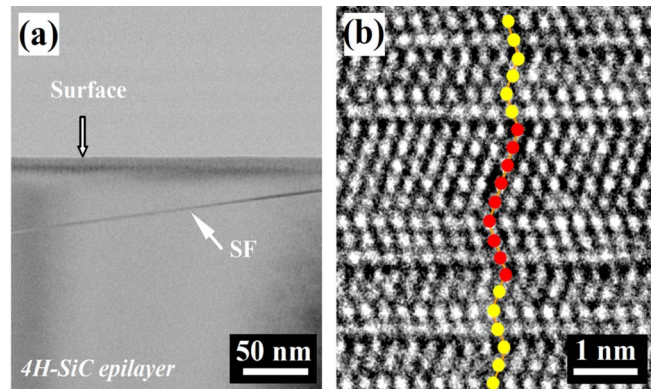


FIG. 3. (Color online) (a) Bright-field TEM image and (b) high-resolution lattice image of a cross section of 4H-SiC epilayer with a SF.

one SF was observed. So the structure of SF obtained here should be the intrinsic feature not affected or interacted with other defects. Figure 3(b) shows the high-resolution TEM image of the SF. The stacking sequence of the SF shown in Fig. 3(b) is (3,5) in the Zhdanov’s notation, which apparently differs from the perfect 4H-SiC, (2,2).

A common formation mechanism of SFs in SiC polytypes is by shear, where part of the crystal above the shear plane is rigidly shifted by the vector connecting the A, B, or C locations in the basal plane. The SFs caused by the shear are called Shockley faults. Starting from the perfect 4H polytype, one can produce two different types of stacking sequences by shear of each one of *h* and *c* bilayers in the right direction, as shown in Fig. 4. The transformation can be denoted as (2,2) → (1,3) and (2,2) → (3,1) in the Zhdanov’s notation [(3,1) is not shown]. Accordingly, we call these two SFs 1SSFs. If we shear both *h* and *c* bilayers (layer 11 and 10) in the same direction, we can produce a SF called 2SSF. The transformation of 2SSFs can be denoted as (2,2) → (6,2). Also if we continue to shift the lower *h* bilayers (layer 7) in the right direction, we will obtain a stacking sequence of (1,7), which was called triple Shockley SFs (3SSFs) by Iwata.¹⁸ However, if we shift the lower *c* bilayer (layer 8) of a 2SSF in the opposite direction (the left direction), as shown in Fig. 4, a new type of 3SSF can be formed. The stacking sequence of the 3SSF is (3,5), exactly the same as that of the SF observed by high-resolution TEM in Fig. 3(b). Therefore, we can identify the SFs with an emission

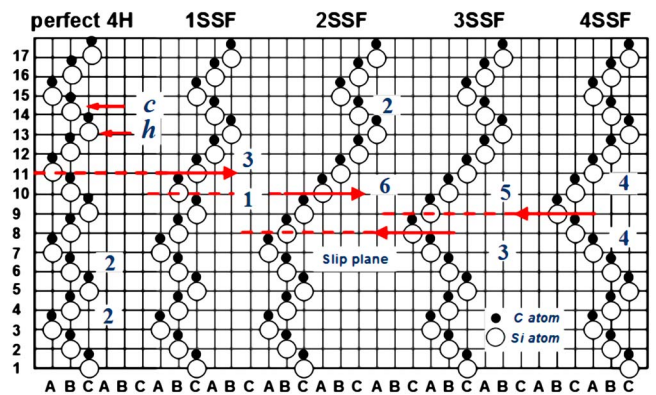


FIG. 4. (Color online) Schematic of the stacking sequences of the Shockley type SFs viewed from the [1120] direction. Stacking sequences are illustrated in terms of the ABC and Zhdanov’s notations.

wavelength of 480 nm as a 3SSF. Furthermore, for 3SSFs (3,5), if we continue to shift the *c* site bilayers (layer 9) in the left direction, we will produce the stacking sequence of 4SSFs (4,4), which coincides with the stacking sequence of the widely reported in-grown 8*H* SFs. As we reported in the previous paper, the 4SSFs tend to be formed during the step-flow epitaxial growth, since only three bilayers are faulted, and the other bilayers exactly followed the substrate.¹⁵ A uniform dimension of the 4SSFs observed in the 4*H*-SiC epilayers, indicates a contemporaneous disturbance (The length of the 4SSFs along the $[11\bar{2}0]$ off-direction corresponds to the projected length of the basal plane in the epilayers), i.e., generated together at the beginning of the epitaxial growth. However, 3SSFs (3,5), observed in 4*H*-SiC epilayers, showed various lengths along the step flow direction within one sample. The width of 3SSFs vertical to the step flow direction is always smaller than that of 4SSFs. This may be a hint that the nucleation process of 3SSFs is different from the 4SSFs.

Regarding the SF formation, the real epitaxial growth (including the initial stage) and the cooling-down processes are important. The cooling stage can also be regarded as an annealing process. The SFs, especially the 2SSFs, are known to be generated after high temperature annealing,⁹ besides being observed in as-grown 4*H*-SiC epilayers. The decrease in electronic energy based on the quantum well model and the strain relaxation was proposed to give rise to the force to shear the basal planes resulting in the generation of 2SSFs.¹³ The PL peak energy of 3SSFs (2.58 eV) is slightly larger than that of 2SSFs (2.48 eV), but lower than 1SSFs (2.95 eV) and 4SSFs (2.70 eV). This means that 3SSFs are more stable than 1SSFs and 4SSFs, similar to 2SSFs. Therefore, it may be reasonable to propose that 3SSFs can be nucleated in both real epitaxial growth and cooling stages to reduce the system free energy. Further investigations on the nucleation process of 3SSFs are required in order to establish a complete model for the formation of 3SSFs.

In summary, strong PL luminescence at room temperature with a characteristic peak at 480 nm was observed in the 4*H*-SiC epilayer's faulted area. The triangular shape of this fault was revealed by monochromatic micro-PL intensity mapping at 480 nm. The lattice stacking sequence of the faulted area was determined as (3,5), which is consistent with the 3SSFs.

This work was supported in part by the Global COE Program (C09) from the Ministry of Education, Culture, Sports, Science and Technology, Japan.

- ¹H. Matsunami and T. Kimoto, *Mater. Sci. Eng. R.* **20**, 125 (1997).
- ²M. Skowronski and S. Ha, *J. Appl. Phys.* **99**, 011101 (2006).
- ³M. H. Hong, A. V. Samant, and P. Pirouz, *Philos. Mag. A* **80**, 919 (2000).
- ⁴K. Maeda, K. Suzuki, S. Fujita, M. Ichihara, and S. Hyodo, *Philos. Mag. A* **57**, 573 (1988).
- ⁵H. Gottschalk, G. Patzer, and H. Alexander, *Phys. Status Solidi A* **45**, 207 (1978).
- ⁶S. Takeuchi, K. Suzuki, K. Maeda, and H. Iwanaga, *Philos. Mag. A* **50**, 171 (1984).
- ⁷S. Izumi, H. Tsuchida, I. Kamata, and K. Izumi, *Appl. Phys. Lett.* **86**, 202108 (2005).
- ⁸H. Fujiwara, T. Kimoto, T. Tojo, and H. Matsunami, *Appl. Phys. Lett.* **87**, 051912 (2005).
- ⁹K. Irmscher, J. Doerschel, H.-J. Rost, D. Schulz, D. Siche, M. Nerding, and H. P. Strunk, *Eur. Phys. J. Appl. Phys.* **27**, 243 (2004).
- ¹⁰R. S. Okojie, M. Xhang, P. Pirouz, S. Tumakha, G. Jessen, and L. J. Brillson, *Appl. Phys. Lett.* **79**, 3056 (2001).
- ¹¹J. P. Bergman, H. Lendenmann, P. A. Nilsson, U. Lindefelt, and P. Skytt, *Mater. Sci. Forum* **353-356**, 299 (2001).
- ¹²J. Q. Liu, M. Skowronski, C. Hallin, R. Söderholm, and H. Lendenmann, *Appl. Phys. Lett.* **80**, 749 (2002).
- ¹³T. Kuhr, J. Q. Liu, H. J. Chung, and M. Skowronski, *J. Appl. Phys.* **92**, 5863 (2002).
- ¹⁴N. Hoshino, M. Tajima, T. Nishiguchi, K. Ikeda, T. Hayashi, H. Kinoshita, and H. Shiomi, *Jpn. J. Appl. Phys., Part 2* **46**, L973 (2007).
- ¹⁵G. Feng, J. Suda, and T. Kimoto, *Appl. Phys. Lett.* **92**, 221906 (2008).
- ¹⁶S. Juillaguet, M. Albrecht, J. Camassel, and T. Chassagne, *Phys. Status Solidi A* **204**, 2222 (2007).
- ¹⁷T. Kimoto, S. Nakazawa, K. Hashimoto, and H. Matsunami, *Appl. Phys. Lett.* **79**, 2761 (2001).
- ¹⁸H. Iwata, U. Lindefelt, S. Öberg, and P. R. Briddon, *J. Appl. Phys.* **93**, 1577 (2003).